IEICE TRANS. FUNDAMENTALS, VOL.E87–A, NO.10 OCTOBER 2004

PAPER Special Section on Wide Band Systems

Application of Adaptive Modulation for Road-to-Vehicle Communication System and Its Improved Effect in Shadowing Duration

Masataka IMAO[†a)], ***Student Member***, **Katsutoshi TSUKAMOTO**[†], ***Member***, ***and*** **Shozo KOMAKI**[†], ***Fellow***

SUMMARY In the road-to-vehicle communication (RVC) on intelligent transport systems (ITS), the frequent occurrence of shadowing caused by other vehicles deteriorates wireless transmission quality because of a small sized zone. However, a diffraction wave generated at the edge of vehicle can be utilized in applying adaptive modulation method with decreased modulation level. Therefore, it can be expected to keep communication only with a diffraction wave under shadowing. Hence this paper proposes an application of adaptive modulation for RVC system. This paper first reveals its improved effect in shadowing duration by computer simulation considering practical traffic flow, radio reflection and diffraction, and then shows that applying adaptive modulation can increase throughput performance largely.

key words: *road-to-vehicle communication (RVC), shadowing, radio diffraction, adaptive modulation, random traffic flow*

1. Introduction

Intelligent transport systems (ITS) is placed on the most important multimedia infrastructures on a road transportation system recently, and it is especially expected to support a safety drive, improve environmental issues caused by traffic congestion, and seamlessly transmit driver's required data including entertainment contents. To achieve these broadband wireless multimedia services, road-to-vehicle wireless communication (RVC) system is an essential technology. In the RVC system, the received signal power at a traveling vehicle largely and rapidly varies because of multipath fading and shadowing. Especially, the frequent occurrence of shadowing caused by other vehicles deteriorates wireless service quality because the vehicle has to access in a small sized zone. To overcome shadowing, some approaches have proposed in Refs. [1] and [2].

The adaptive modulation method [3], which switches modulation level adaptively according to the quality of wireless link, can equivalently decrease the required carrier-to-noise power ratio (CNR), and maintain communication under the environment of low received power. This method is applied or assumed to various systems such as high data rate (HDR) [4], wideband code division multiple access (W-CDMA) [5], and dedicated short-range communication (DSRC) system [6], [7]. We focus the characteristics of adaptive modulation method on the shadowing environment in RVC system. In the environment of shadowing, a traveling vehicle can obtain weak power from a diffraction wave diffracts at the edge of other vehicle in spite of blinding direct path. Hence it can be expected to keep communication only with a diffraction wave under shadowing if applying the adaptive modulation method to RVC and utilizing the power of diffraction wave. However, Refs. [1] and [2] have never been examined about the effectiveness of diffraction wave in RVC. Furthermore, though Refs. [6] and [7] consider to apply the adaptive modulation method to DSRC, it has investigated under the ideal conditions such as 2-ray propagation model considering only a direct path and a ground-reflection path with single vehicle, and it has not mentioned about the improvement effect of shadowing.

Therefore, this paper proposes an application of adaptive modulation method for RVC system to use the weak power of diffraction wave. To perform the investigation for the application effect of adaptive modulation, we have to consider some practical traffic flows and multipath environments with radio reflection and diffraction. Hence this paper first reveals the utilizing effect of diffraction wave in shadowing duration by computer simulations, and then shows the application effect of adaptive modulation method in throughput performance.

This paper is organized as followings. In Sect. 2, the traffic flow parameters that characterize random traffic flow are described, and a statistical model of traffic flow is introduced. Section 3 introduces the radio propagation model considering direct path, reflection path, and diffraction wave. Section 4 discusses a characteristic of received signal power under the practical traffic environment, and Sect. 5 shows some computer simulation results of the statistical characteristics of shadowing duration and the throughput characteristics with or without adaptive modulation. Finally, Sect. 6 concludes this paper.

2. Statistical Model of Traffic Flow

Figure 1 shows the statistical model of vehicle traffic considered in this paper. This model assumes the road with three lanes which are named as lane 1, 2, and 3 shown in Fig. 1. We assume to use 5.8 GHz as a frequency band, and the BSs are placed at even intervals to realize continuous communication. The BS interval shows the length between two adja-

Manuscript received February 23, 2004.
Manuscript revised May 15, 2004.
Final manuscript received June 21, 2004.

[†]The authors are with the Department of Communications Engineering, Graduate School of Engineering, Osaka University, Suita-shi, 565-0871 Japan.
a) E-mail: imao@roms.comm.eng.osaka-u.ac.jp

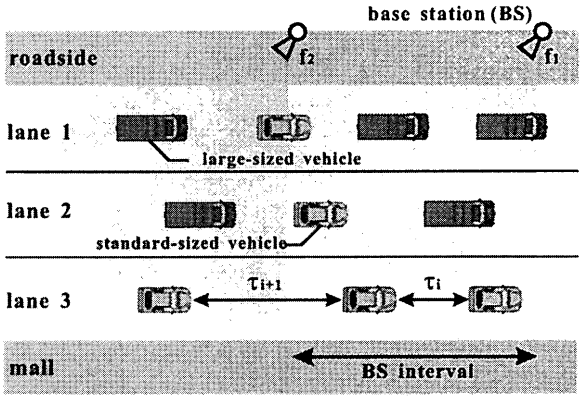

Fig. 1 Statistical model of traffic flow.

cent BSs, and we assume its interval of 50 m or 100 m in this model. Also we assume that the interference between adjacent BSs can be ignored by the use of different frequency in each communication zone such as f_1 and f_2 shown in Fig. 1 [8].

This model introduces following parameters to characterize traffic flow: First parameter is vehicle speed, v, at each lane. It is assumed that the vehicle speed is constant and same among vehicles. Second one is time headway, τ_i, between two vehicles in the same lane. Erlang distribution is introduced as the probability density function of the time headway between vehicles, τ_i, shown in Fig. 1. The probability density function of Erlang distribution is given by

$$p(\tau_i) = \frac{(k\mu)^k}{(k-1)!}\tau_i^{k-1}e^{-k\mu\tau_i}, \tag{1}$$

where μ and k are the mean value of time headway and Erlang phase, respectively. Erlang distribution is usually used to express the statistics of practical traffic flow instead of exponential distribution (i.e., Poisson traffic flow) [9]. The Erlang phase, k, indicates the degree of the randomness of the traffic flow, which decreases as k increases. The third important parameter is the ratio of the number of different type of vehicle to the total number of vehicle. This paper considers two types of vehicle, large-sized vehicle and standard-sized vehicle, and introduces the ratio of the number of the large-sized vehicle to the total number of vehicles at each lane, which is called the large-sized vehicle ratio (LVR).

3. Radio Propagation Model

Figure 2 illustrates the radio propagation model considering radio reflection at other vehicles and ground, and diffraction at other vehicles. This model assumes that a rectangular horn antenna is equipped as both a roadside antenna at base station (BS) and an in-vehicle antenna at mobile station (MS), and also assumes that the tilt angle of the BS antenna is 30 degrees against the land surface as shown in Fig. 2.

When the target vehicle receives the power from a direct, ground-reflection, and/or vehicle-reflection path, the total received power P_{d+r} is given by

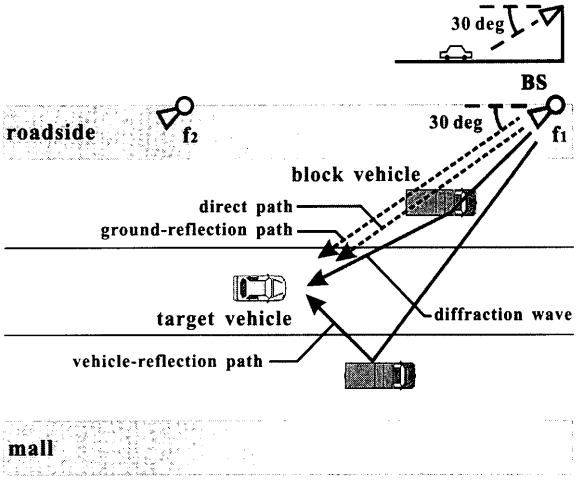

Fig. 2 Radio propagation model.

$$P_{d+r} = \begin{cases} aP_t + G_t + G_r \\ +10\log_{10}\left\{D_d\left(\frac{\lambda}{4\pi r_d}\right)\right\}^2 \quad (\equiv P_d) \\ \qquad (w/o\ reflection path) \\ P_t + G_t + G_r \\ +10\log_{10}\left\{\left|D_d\left(\frac{\lambda}{4\pi r_d}\right)\right. \right. \\ \left. \left. + \sum_{i=1}^{n} D_{l_i}R_{l_i}\left(\frac{\lambda}{4\pi r_{l_i}}\right)e^{\{-j\frac{2\pi}{\lambda}(r_{l_i}-r_d)\}}\right|^2\right\} \\ \qquad (w/\ \ reflection path) \end{cases} \tag{2}$$

where P_t [dBm] is the transmitted power, G_t [dB] and G_r [dB] are the antenna gains at BS and MS. D_d and D_l are the directivity gains for direct and reflection path, respectively. r_d and r_l are the path length of direct and reflection path, and R_l and λ are the reflection coefficient and wavelength [10]. Notice that n is the number of the reflection path including the ground-reflection path and the vehicle-reflection path via the vehicles around the target vehicle. Though the received power from the paths reflecting more than two times becomes often large, these paths seldom exist because such paths are determined uniquely by the geometrical relationship among BS, MS, and the vehicle position at reflection point, and this situation hardly occurs due to its low probability. Hence we ignore the multiple reflection paths.

The direct path to the target vehicle is often blind due to other vehicles, but the target vehicle obtain the received power from diffraction wave which arises from the diffraction at the edge of the block vehicle. The single knife-edge propagation model known as a simple diffraction model [11], [12] is shown in Fig. 3. We assume to ignore any other paths diffracting twice or more times because the received power from multiple diffraction wave is enough low compared to that of single knife-edge diffraction wave [13]. Hence the received power of the diffraction wave can be represented as

$$P_{diff} = P_d - P_{att}, \tag{3}$$

where P_d is the power from direct path which is given by upper term of Eq. (2), and P_{att} is the knife-edge attenuation which is given by

$$P_{att} = -10\log_{10}\left[\frac{1}{2}\left\{\frac{1}{2} + C^2(\nu) - C(\nu) + S^2(\nu) - S(\nu)\right\}\right], \tag{4}$$

where $C(\nu)$ and $S(\nu)$ are the Fresnel cosine and sine integrals, respectively. Notice that the parameter ν is the clearance coefficient, which can be expressed in terms of the geometrical parameters defined in Fig. 3 as

$$\nu = h_e\sqrt{\frac{2(d_1 + d_2)}{\lambda d_1 d_2}}, \tag{5}$$

where h_e is the excess height of the edge. The knife-edge attenuation P_{att} versus the clearance coefficient ν is shown in Fig. 4. The received power from diffraction wave is enough low compared to that of the direct or reflection path and this fact has confirmed not only on the case shown in Fig. 5 but also on the all case in our simulations. Therefore the effect of fluctuation caused by the interference between direct or reflection path and diffraction wave can be ignored, and the total received power P_R is given by

$$P_R = P_{d+r} + P_{diff}, \tag{6}$$

and the received CNR γ is given by

$$\gamma = \frac{P_R}{N_t} = \frac{P_R}{\kappa TBF}, \tag{7}$$

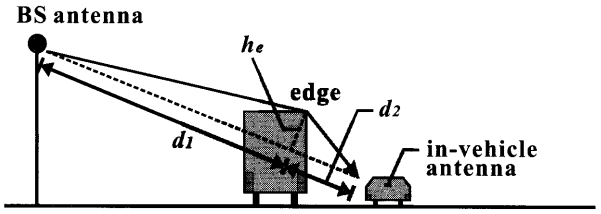

Fig. 3 Knife-edge diffraction model.

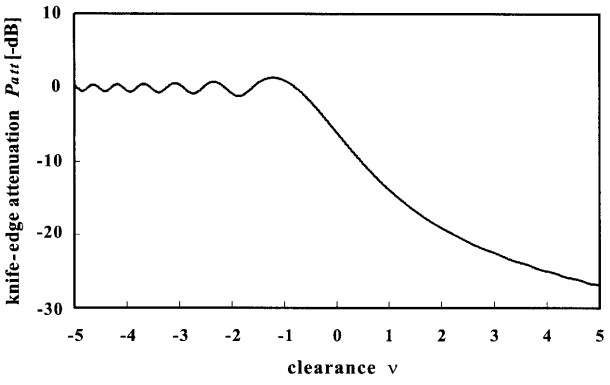

Fig. 4 Knife-edge attenuation.

where N_t is the thermal noise at MS, and κ, T, B, F are the Boltzmann constant, the temperature, the frequency bandwidth, and the noise figure, respectively. We assume that the modulation level is switched by the γ. Note that the thermal noise power at MS is assumed to be equal.

4. Characteristics of Reflection and Diffraction Wave at Vehicles

Figure 5 shows the example of the received signal power of a target vehicle versus its position on lane 2. Note that the BS is placed every at 50 m, and its height and transmitted power are 6 m and 10 dBm, respectively.

This figure can divide into 3 distinctive regions, an region A, B, and C. If ignoring the power of diffraction wave, no received power can be obtained at the target vehicle in the region A because the block vehicle on lane 1 shadows the BS antenna. As shown in Fig. 5, however, the target vehicle can receive power of the diffraction wave in the region A continuously. Since the received power of the diffraction wave may be low extremely compared to the power from direct path, it is expected the target vehicle can combat shadowing when reducing the required power by using a higher reliable modulation format. Next, in the region B, the received power from the vehicle-reflection path which reflects

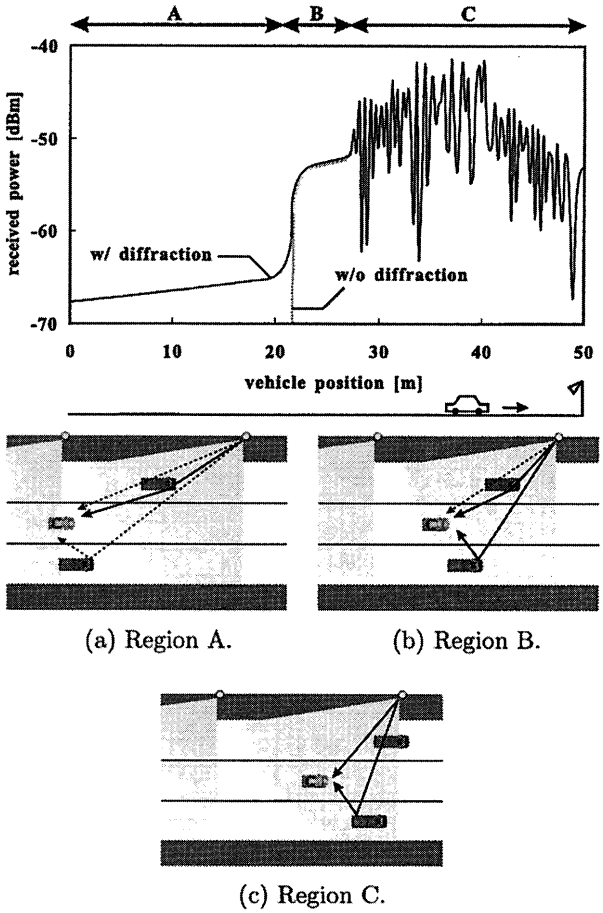

Fig. 5 The effect of vehicle-reflection path and diffraction wave.

at the vehicle on lane 3 is quite strong, hence it is expected that the target vehicle enables to achieve high-rate communication by using a higher-level modulation format. When the target vehicle moves into the region C and the no other vehicles shadow the BS antenna, the target vehicle can obtain the received power from a direct and a ground-reflection path well.

These examples show that an adaptive multi-level quadrature amplitude modulation (QAM) method can use the weak power of a diffraction wave, and it will be greatly effective to combat the shadowing and to achieve a high-rate communication in RVC system.

5. Simulation Results

In this section, we investigate the reduction effect of the reflection path and diffraction wave in the shadowing duration, and the throughput when the adaptive modulation is employed for RVC. The shadowing is defined as the situation that the CNR with coherent detection is less than the required CNR that is given by the required bit error rate (BER). Also an ideal phase synchronization is assumed under the multipath fading or Doppler frequency shift in the RVC system.

Table 1 shows the system model parameters used in simulations. In these simulations, we assume the use of the same frame format as that of DSRC standard (ARIB STD-T75) [14], and its frame length and the modulation changing cycle are 4 msec and 100 msec, respectively. Furthermore, a time division multiple access/frequency division duplex (TDMA/FDD) is applied as the access method that is defined in ARIB STD-T75, and it is assumed that the modulation level in each time-slot can be switched independently [9].

Table 1 System model parameters (STD = Standard-sized vehicle, LRG = Large-sized vehicle).

Transmitted frequency f		5.8 GHz
Transmitted power P_t		10 dBm
BS/MS antenna (aperture)		Rectangular horn (5 cm)
BS/MS antenna gain G_t, G_r		10/5 dBi
Bandwidth B		5 MHz
Noise figure at MS F		10 dB
Multiple access method		TDMA/FDD
Frame length		4 msec
Modulation changing cycle		100 msec
Maximum bit rate (QPSK)		4 Mbps
Required BER		10^{-5}
Required CNR	QPSK	12.6 dB
	16 QAM	19.5 dB
	64 QAM	25.6 dB
Lanes		3
Vehicle types		Standard-sized/Large-sized
Lane width		4.0 m
Roadside width		2.0 m
Reflection coefficient R_l	ground	0.8
	vehicle	0.9
Vehicle length		(STD) 4.5 m (LRG) 10.0 m
Vehicle width		(STD) 2.5 m (LRG) 2.5 m
Vehicle height		(STD) 1.5 m (LRG) 4.0 m
Dashboard height		(STD) 1.0 m (LRG) 2.5 m

We assume the road with three lanes as shown in Fig. 1, and two types of traffic conditions; the free flow and the congested flow, are performed in computer simulations. Table 2 shows the traffic flow parameters. In the free flow condition, the vehicle speed on lane 1 is set to be the lowest value, and its Erlang phase and LVR are set to be the highest value. Therefore, its traffic randomness is the least of three lanes. On the other hand, in the congested flow condition, the vehicle speed, Erlang phase, and LVR are similar on all lanes.

5.1 Shadowing Duration

The communication quality of RVC system largely depends on the frequency of shadowing. Figures 6–9 show the cumulative distribution of the shadowing duration of standard-sized vehicle under the free flow and congested flow, and Table 3 shows the mean shadowing duration when the BS interval is 100 m. Notice that the γ_{req} in Table 3 means the required CNR.

Comparison between traffic flows

It is found from Figs. 6–9 that the shadowing duration in the situation of congested flow is about 1 order longer than that in the situation of free flow. This is because that, once the target vehicle moves into the shadow of a large-sized vehicle, a long-time shadowing occurs more frequent in the situation of the congested flow because of the smallness of speed difference between lanes.

Table 2 Traffic flow parameters.

Lane		1	2	3
Free flow	Vehicle speed [km/h]	80	90	100
	Mean time headway [sec]	4.0	3.0	2.0
	Erlang phase	4	3	2
	LVR [%]	70	50	30
Congested flow	Vehicle speed [km/h]	10	15	20
	Mean time headway [sec]	5.0	5.0	5.0
	Erlang phase	6	6	6
	LVR [%]	50	40	30

Table 3 Mean shadowing duration [sec] (BS interval =100 m).

(a) Free flow.

BS height	5 m		10 m	
γ_{req}	12.6 dB	25.6 dB	12.6 dB	25.6 dB
Lane 1	0.011	0.101	0.006	0.059
Lane 2	0.291	0.421	0.017	0.122
Lane 3	0.436	0.572	0.227	0.285

(b) Congested flow.

BS height	5 m		10 m	
γ_{req}	12.6 dB	25.6 dB	12.6 dB	25.6 dB
Lane 1	1.84	4.66	1.12	5.39
Lane 2	5.06	8.08	0.99	4.81
Lane 3	7.06	9.59	4.62	4.65

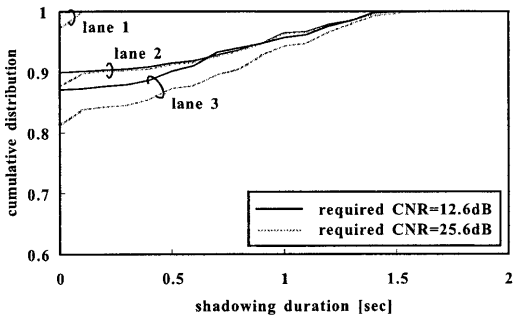

(a) BS interval =50m.

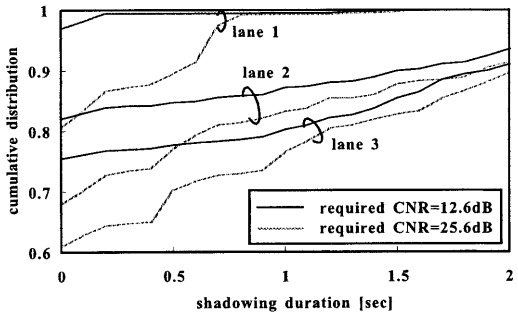

(b) BS interval =100m.

Fig. 6 Shadowing duration (BS height =5 m, Free flow).

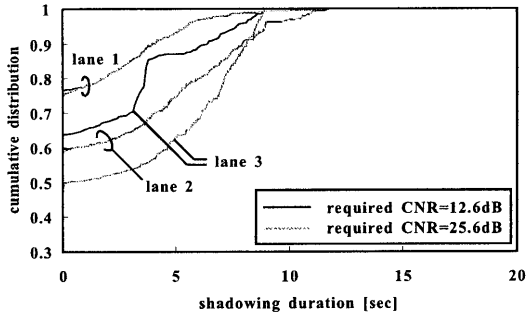

(a) BS interval =50m.

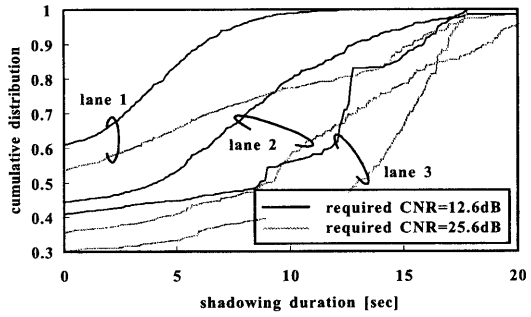

(b) BS interval =100m.

Fig. 8 Shadowing duration (BS height =5 m, Congested flow).

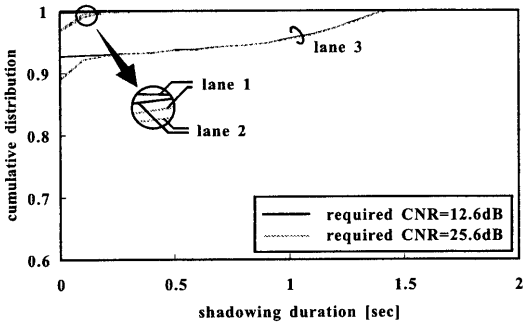

(a) BS interval =50m.

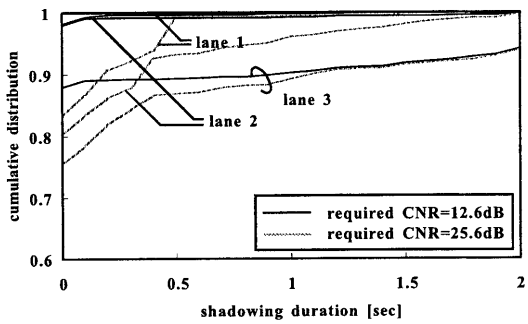

(b) BS interval =100m.

Fig. 7 Shadowing duration (BS height =10 m, Free flow).

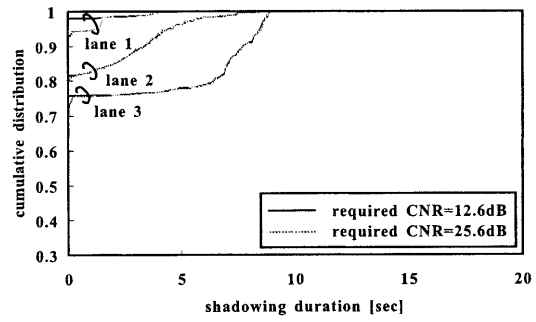

(a) BS interval =50m.

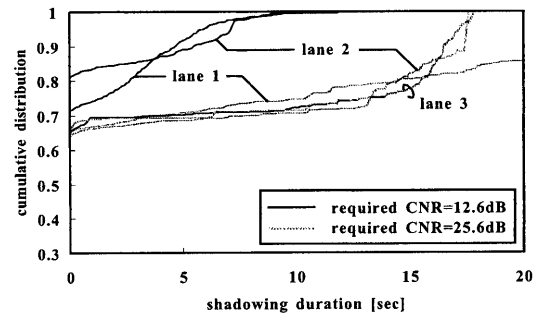

(b) BS interval =100m.

Fig. 9 Shadowing duration (BS height =10 m, Congested flow).

Comparison between BS intervals

It is also found from each of Figs. 6–9 that decreasing the required CNR improves the shadowing duration, and its effect is clearer when the BS interval is 100 m compared to when the BS interval is 50 m. This is because the power of diffraction becomes more available when the target vehicle is farther from BS because of frequent shadowing. This improvement can be also found in the mean values of the shadowing duration shown in Table 3 that, when the BS height

is 10 m, the decrease of the required CNR reduces the mean shadowing duration on lane 1 up to its 10% and 20% in the case of free flow and congested flow condition respectively.

Comparison between the required CNRs

It is found from Figs. 6(b) and 7(b) for the BS interval of 100 m in the free flow condition that, the rate of shadowing duration which is less than 1.0 sec can be improved largely in case that the BS height is 5 m and 10 m when the required CNR is reduced from 25.6 dB to 12.6 dB. When the BS height is 5 m shown in Fig. 6(b), the shadowing durations of 99% vehicles become about less than 0.2 sec and 1.0 sec for the required CNR of 12.6 dB and 25.6 dB on lane 1, respectively. This result leads that the received power of diffraction wave becomes more available in the case of short-time shadowing than the case of long-time shadowing.

Comparison between lanes

From Figs. 6 and 8 in the case of the free flow and the congested flow condition that, when the BS height is low, the long-time shadowing occurs more frequent on lane 3 than lane 1 and 2. This reason is that the occurrence of shadowing on lane 2 depends on the LVR on lane 1, and the occurrence of shadowing on lane 3 depends on the LVR both on lane 1 and 2. On the other hand, in the case of high BS antenna shown in Figs. 7 and 9 that, the in-vehicle antenna of target vehicle on lane 2 is not shadowed by the large-sized vehicles on lane 1 because of their geometrical relationship, and shadowed only by the vehicle traveling forward on the same lane. Hence the characteristics of shadowing duration on lane 2 become similar to that of lane 1.

These results are also found on the mean values of the shadowing duration in Table 3. In the case that the required CNR is 12.6 dB under the free flow condition, though the mean shadowing duration on lane 2 is about 26 times as long as that on lane 1 when the BS height is 5 m, it becomes similar to that on lane 1 when the BS height is 10 m. This characteristic also appears on the congested flow condition.

On the lane 3 under the free flow and the congested flow condition, however, the long-time shadowing tends to most occur compared to lane 1 and 2. This is because the large-sized vehicles on lane 2 shadow the in-vehicle antenna on lane 3 in spite of heightening the BS height.

From Figs. 6–9, we can also see the probability that the shadowing duration becomes 0 sec. We call it as "clearance rate." Several features about clearance rate are found from Figs. 6–9. First, the clearance rate improves as the BS height becomes high since the probability that the BS is shadowed by the block vehicle becomes less than the case when the BS height is low. Second, the clearance rate deteriorates as the BS interval increases because the amount of vehicles between the BS and the target vehicle become increases, and also the possibility that the block vehicle shadows the BS height becomes high. Otherwise, the improvement effect of clearance rate is achieved as reducing required CNR and its effect is longer when the BS interval is 100 m compared to when the BS interval is 50 m. This is because shadowing occurs more frequent as the target vehicle is farther from the BS, and the power of diffraction wave becomes more available in this case.

5.2 Throughput Performance

In Sect. 5.1, it was investigated that the performance of shadowing duration was largely improved by decreasing the required CNR and utilizing the power of diffraction wave.

When employing the adaptive modulation to RVC system, the required CNR can be reduced and the power of diffraction wave can be used effectively. However, the throughput becomes low since the data rate decreases as the required CNR decreases. Hence we must be investigated the throughput performance. Notice that the throughput is defined as the received data size per second in the environment of practical traffic flow.

We assume the adaptive modulation with quadrature phase shift keying (QPSK), 16 QAM, and 64 QAM. The modulation level is adaptively switched according to the received CNR. Since the required BER is 10^{-5} at $\pi/4$-shift QPSK modulation method with 4Mbps in ARIB STD-T75, the required BER in the simulation is the same value of 10^{-5}, and each of the required CNR of QPSK, 16 QAM, and 64 QAM is shown in Table 1.

Figures 10–13 show the throughput distribution of standard-sized vehicle under the free flow and the congested flow, respectively, and Table 4 shows the mean throughput when the BS interval is 100 m. In Figs. 10–13, "QPSK" and "64 QAM" mean that it is assumed to use QPSK and 64 QAM as the fixed modulation method, respectively, and "adaptive" means to assume to use QPSK, 16 QAM, and 64 QAM adaptively according to the received CNR.

As mentioned before, we assumed the modulation changing cycle of adaptive modulation was 100 msec in these simulations. Since the strength of received signal varies with the period less than this modulation changing cycle in the region C as shown in Fig. 5, the MS selecting higher-level modulation suffers some bit errors in this region. The throughput performances shown in Figs. 10–13 were obtained considering these bit errors. Hence, these simulations examined the availability of the adaptive modulation under the condition of the relative long value of the modulation changing cycle. However, the selection of modulation changing cycle strongly depends on the variation speed of received signal strength. Therefore, if it is able to realize the shorter changing cycle which is comparable to the signal variation, more improvement in throughput performance will be expected.

Differences between traffic flows

From Figs. 10 and 11, for free flow condition, the target vehicle becomes difficult to achieve maximum through-

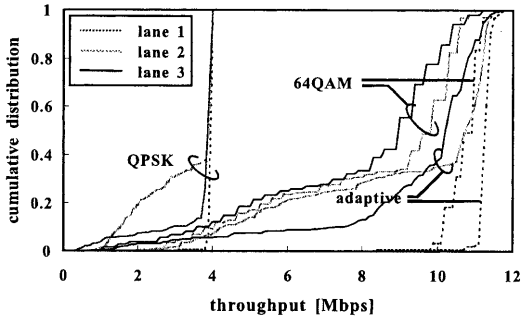

(a) BS interval =50m.

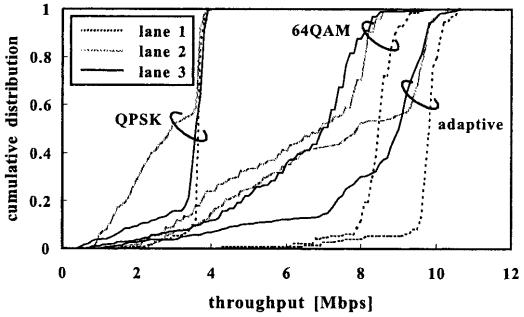

(b) BS interval =100m.

Fig. 10 Throughput (BS height =5 m, Free flow).

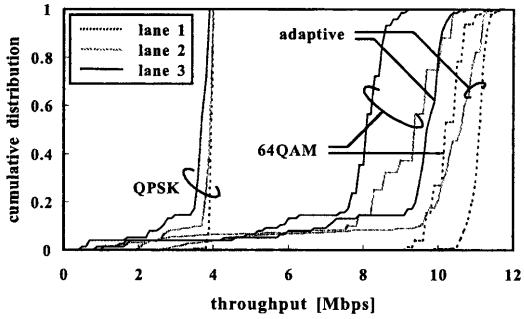

(a) BS interval =50m.

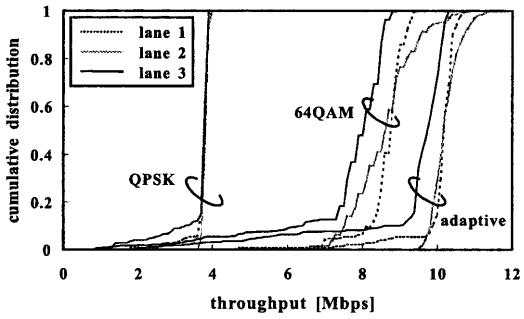

(b) BS interval =100m.

Fig. 11 Throughput (BS height =10 m, Free flow).

put as increase as the multi-level number of QAM. This is because the target vehicle cannot obtain enough power to receive high-level QAM, and long-time shadowing occurs frequently. Otherwise, the target vehicle tends to achieve high-rate throughput easily when using the adaptive modulation, and the mean throughput increases up to 1.3 times compared to that of case using fixed 64 QAM as shown in Table 4. The reason is that the received power from diffraction wave is available as decreasing the modulation level when the shadowing occurs, and the target vehicle can keep communication continuously.

Table 4 Mean throughput [Mbps] (BS interval =100 m).

(a) Free flow.

BS height	5 m		10 m	
γ_{req}	64 QAM	adaptive	64 QAM	adaptive
Lane 1	8.44	9.74	8.68	10.12
Lane 2	6.19	7.31	8.62	10.26
Lane 3	6.36	8.26	7.66	9.38

(b) Congested flow.

BS height	5 m		10 m	
γ_{req}	64 QAM	adaptive	64 QAM	adaptive
Lane 1	7.21	8.52	7.38	8.80
Lane 2	5.06	6.11	8.40	9.89
Lane 3	4.04	6.00	6.42	8.03

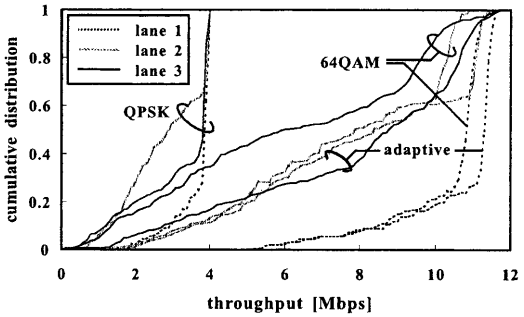

(a) BS interval =50m.

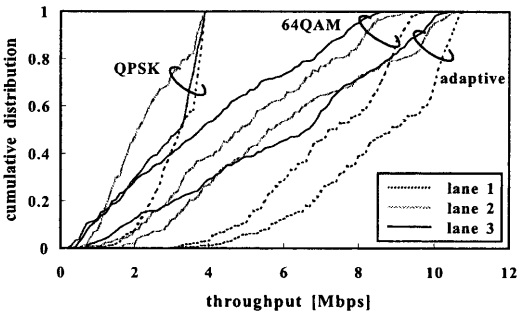

(b) BS interval =100m.

Fig. 12 Throughput (BS height =5 m, Congested flow).

Next, from Figs. 12 and 13 that, for congested flow condition, the throughput distributes from 0 Mbps to maximum throughput uniformly for both case of the adaptive modulation and the fixed modulation when the BS height is 5 m. The reason is that, when the target vehicle moves into "deep shadow" of block vehicle, the received power is too low to appear the improvement effect of throughput though the multi-level number of QAM decreases. However, when the BS height is heightened to 10 m, the frequency of low-rate throughput is improved particularly by

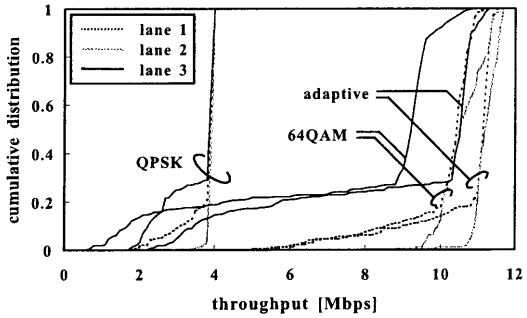

(a) BS interval =50m.

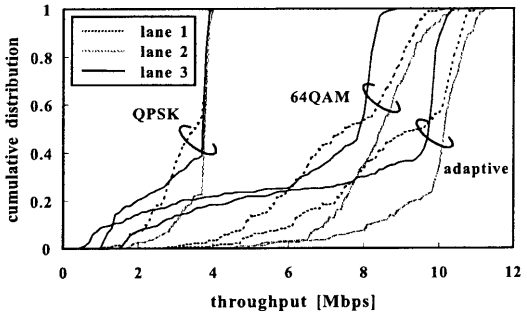

(b) BS interval =100m.

Fig. 13 Throughput (BS height =10 m, Congested flow).

using the adaptive modulation method shown in Fig. 13, and the mean throughput increases about 1.25 times compared to that of case using fixed 64 QAM.

Quantitatively, from Figs. 10(a) and 12(a), 90% of vehicles can achieve throughput more than 5 Mbps and 8 Mbps when using fixed 64 QAM and the adaptive modulation method, respectively, in the free flow condition. On the other hand, 90% of vehicles can achieve throughput more than 1.5 Mbps and 3 Mbps when using fixed 64 QAM and the adaptive modulation method, respectively, in the congested flow condition. These results show that, the absolute value of throughput is small, but its improvement effect of throughput by applying the adaptive modulation method is largely under the congested flow condition.

Differences between lanes

It is found from Figs. 10 and 12, when the BS height is low, the throughput performance between lanes are different largely. However, the vehicles can obtain stable throughput such as concentrating near to maximum throughput on all lanes when heightening the BS height shown in Figs. 11 and 13 because of decreasing the occurrence of shadowing. This result shows that heightening the BS height and using the adaptive modulation can be achieved high-rate and stable data transmission on all lanes.

5.3 Relationship between BS Interval and Received Data

The expansion of the BS interval causes two effects: one is that the communication area for each vehicle can be extended, and the other is that the data size which is received by each vehicle will be reduced because of increasing the amount of vehicles in the communication area. Hence the mean received data size of a vehicle should be investigated against the BS interval.

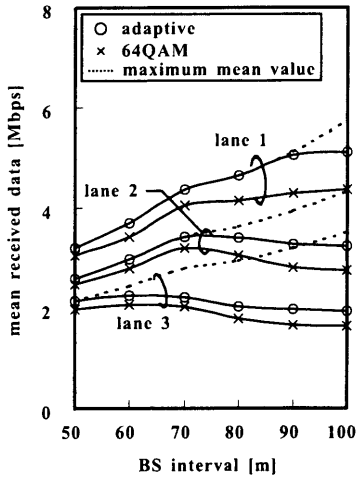

(a) BS height =5m.

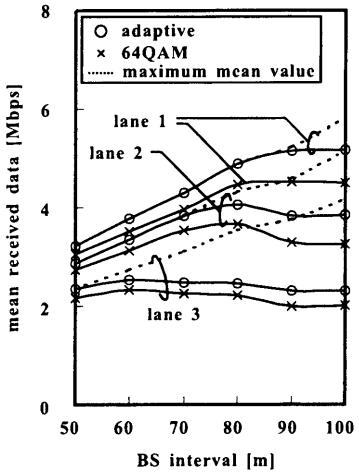

(b) BS height =10m.

Fig. 14 Mean received data size (Free flow).

Figures 14 and 15 show the mean received data size of a vehicle under the condition of free flow and congested flow. Note that broken line in Fig. 14 shows the maximum mean received data size of a vehicle using adaptive modulation. It is found from these figures that the adaptive modulation can improve the mean received data size as increasing the BS interval. This is because shadowing occurs more frequent as the target vehicle is farther from BS and the power of diffraction wave is more available.

In the case of the free flow condition, Fig. 14 shows that the maximum mean received data size is achieved when the BS interval is about 100 m on lane 1, about 70 m on lane 2, and about 60 m on lane3, respectively. This means that as the vehicle density increases, the BS interval that maximizes the mean received data size decreases. On the other hand, from Fig. 15 that, in the case of congested flow, the mean

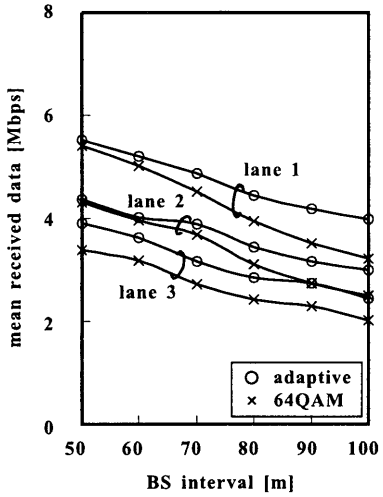

(a) BS height =5m.

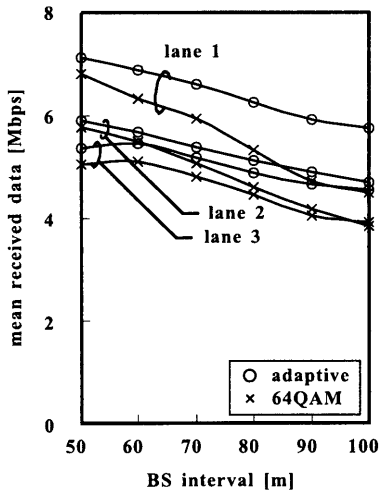

(b) BS height =10m.

Fig. 15 Mean received data size (Congested flow).

received data size decreases uniformly as the BS interval increases from 50 m to 100 m because of the highness of the vehicle density. Since the BS interval that optimizes the mean received data size strongly depend on the condition of traffic flow, it needs to design the BS arrangement with the forecast of traffic conditions.

6. Conclusions

In this paper, we have proposed an application of adaptive modulation to improve shadowing duration performance for RVC system for high-rate communication. We have investigated the shadowing duration, clearance rate, and the throughput in the RVC employing the adaptive modulation method by computer simulations considering direct, reflection path and diffraction wave.

From simulation results, we have found followings:

- The diffraction wave has enough power to improve the shadowing duration when decreasing the required CNR, and the shadowing duration less than 1.0 sec can be improved largely when the required CNR is reduced from 25.6 dB to 12.6 dB.
- The adaptive modulation improves the probability that the throughput drops to the low value by using the power of diffraction wave effectively, and the mean throughput increases 1.3 and 1.25 times as large as comparing to that of the case using fixed 64 QAM in the case of the free flow and the congested flow condition, respectively.
- It is found that, in the condition of the free flow, there exists the optimum BS interval to maximize the mean received data size, and its optimum BS interval is 60–100 m.

It needs to consider the feedback control and its control delay for modulation switching to employ the adaptive modulation, and this will be one of our further studies.

Acknowledgement

This paper is partially supported by the Grant-in-Aid for Scientific Research (B) No.14350202, from the Japan Society for the Promotion of Science.

References

[1] R. Fukui, N. Kakita, T. Yashiro, H. Shigeno, and Y. Matsushita, "A practically evaluation of road-to-vehicle communication system by the method of constituting a continuous radio zone using road lighting," J. IPSJ, vol.43, no.12, pp.3931–3938, Dec. 2002.
[2] Y. Morita and T. Hasegawa, "On unified road-to-vehicle and inter-vehicle communications for shadowing avoidance," IEICE Technical Report, ITS2002-32, Nov. 2002.
[3] S. Sampei and N. Morinaga, "Adaptive modulation techniques for high-speed wireless data transmission," J. IEICE, vol.85, no.4, pp.245–251, April 2002.
[4] P. Bender, P. Black, M. Grob, R. Padovani, N. Sindhushayana, and A. Viterbi, "CDMA/HDR: A bandwidth-efficient high-speed wireless data service for nomadic users," IEEE Commun. Mag., vol.38, no.7, pp.70–77, July 2000.
[5] M. Sawahashi, K. Higuchi, H. Atarashi, and N. Miki, "High-speed packet wireless access in W-CDMA and its radio link performance," IEICE Trans. Commun. (Japanese Edition), vol.J84-B, no.10, pp.1725–1745, Oct. 2001.
[6] T. Sakamoto and K. Abe, "Performance analysis of adaptive modulation technique on DSRC system," Proc. ITST2002, pp.161–164, Nov. 2002.
[7] H. Ishii and T. Hasegawa, "A study on application of SNR adaptive modulation to DSRC," IEICE Technical Report, ITS99-110, March 2000.
[8] M. Hiraiwa, T. Sakamoto, M. Mori, T. Noake, and T. Nishizawa, "Implementation and evaluation of ARIB STD-T75 based DSRC system," IEICE Trans. Fundamentals (Japanese Edition), vol.J86-A, no.12, pp.1382–1393, Dec. 2003.
[9] M. Katakura, "Time headway distribution of traffic flow," Proc. JSCE, no.189, pp.107–115, May 1971.
[10] N. Taguchi, T. Kimura, T. Horimatsu, A. Kato, and M. Fujise, "Propagation characteristics of 60GHz millimeter wave for ITS inter-vehicle communications (3)—Distance characteristics for antennas with different directivity," Proc. ITST2000, pp.259–262, Oct. 2000.
[11] T. Araki, T. Shimura, and S. Ishiko, "Propagation characteristics of 5.8 GHz road vehicle communication system using multi-

antenna transmission," Proc. Fundamentals Conf. IEICE '98, pp.54–55, Sept. 1998.
[12] S.R. Saunders, Antennas and propagation for wireless communication systems, pp.45–51, John Wiley & Sons, 1999.
[13] Y. Hosoya, Radiowave propagation Handbook, pp.23–27, Realize, 1999.
[14] ARIB, ARIB STD-T75, Sept. 2001.

Masataka Imao was born in Osaka, Japan on September 5, 1978. He received the B.E. and M.E. degrees in Communications Engineering from Osaka University, Osaka, Japan, in 2002 and 2003, respectively. He is currently pursuing the Ph.D. degree at Osaka University, and engaging in the research on radio communication systems. He is a student member of IEEE.

Katsutoshi Tsukamoto was born in Shiga, Japan in October 7, 1959. He received the B.E., M.E. and Ph.D. degrees in Communications Engineering from Osaka University, in 1982, 1984 and 1995 respectively. He is currently an Associate Professor in the Department of Communications Engineering at Osaka University, engaging in the research on radio and optical communication systems. He is a member of IEEE and ITE. He was awarded the Paper Award of IEICE, Japan in 1996.

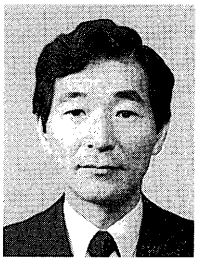

Shozo Komaki was born in Osaka, Japan, in 1947. He received B.E., M.E. and Ph.D. degrees in Electrical Communication Engineering from Osaka University, in 1970, 1972 and 1983 respectively. In 1972, he joined the NTT Radio Communication Labs., where he was engaged in repeater development for a 20-GHz digital radio system, 16-QAM and 256-QAM systems. From 1990, he moved to Osaka University, Faculty of Engineering, and engaging in the research on radio and optical communication systems. He is currently a Professor of Osaka University. Dr. Komaki is a senior member of IEEE, and a member of the Institute of Television Engineers of Japan (ITE). He was awarded the Paper Award and the Achievement Award of IEICE, Japan in 1977 and 1994 respectively.